Sensors and Actuators B 232 (2016) 234–242

Contents lists available at ScienceDirect

Sensors and Actuators B: Chemical

journal homepage: www.elsevier.com/locate/snb

Polymerizing dopamine onto Q-graphene scaffolds towards the fluorescent nanocomposites with high aqueous stability and enhanced fluorescence for the fluorescence analysis and imaging of copper ions

Minmin Dong[a], Chunli Liu[a], Shuying Li[a], Rui Li[a], Yuchun Qiao[a], Liyan Zhang[a], Wei Wei[a], Wei Qi[a], Hua Wang[a,b,*,1]

[a] Shandong Province Key Laboratory of Life-Organic Analysis, College of Chemistry and Chemical Engineering, Qufu Normal University, Qufu, Shandong 273165, PR China
[b] Jining Functional Materials and Surface Treatment Technology R & D Center, Southern Shandong Academy of Engineering Technology, Jining, Shandong 272000, PR China

ARTICLE INFO

Article history:
Received 31 October 2015
Received in revised form 25 March 2016
Accepted 25 March 2016
Available online 26 March 2016

Keywords:
Polymerizing dopamine
Q-graphene scaffolds
Fluorescence enhancement
Fluorescence analysis and imaging
Copper ions

ABSTRACT

Dopamine (DA) was polymerized onto the scaffolds of Q-graphene (QG) nanomaterials by the one-pot H_2O_2 oxidation under the microwave radiations. The so yielded fluorescent QG@PDA nanocomposites could present the high aqueous stability and photostability. Unexpectedly, they could display the enhanced fluorescence and photoluminescence, which are about 1.5-time larger than those of the fluorescent PDA nanoparticles. More importantly, the fluorescence and photoluminescence of QG@PDA nanocomposites could be specifically quenched by Cu^{2+} ions, which could be efficiently restored by using the Cu^{2+}-chelating ligand (i.e., EDTA). The developed fluorimetry was applied to detect Cu^{2+} ions in wastewater with the detection limit down to about 10 nM. The feasibility of the quantitative observations by the fluorescence imaging for Cu^{2+} ions could also be expected. This QG@PDA-based fluorimetry for Cu^{2+} ions is rapid, sensitive, selective, and field-applicable, promising the potential applications in the environmental and industrial fields.

1. Introduction

The pollution of heavy metal ions has concentrated increasing attentions due to their potential damage to the environment and human body. Copper (Cu^{2+}) ions with excess amount in body, which may result from the over uptake of Cu^{2+} ions from water and food, may have long-term adverse effects on liver, kidney, and neurological systems [1,2]. Up to date, many classic analysis technologies have been developed to detect Cu^{2+} ions [3–7], and especially the fluorometric methods have been preferentially applied with some distinct advantages such as high analysis sensitivity, simplicity, and short response time [8,9]. In recent decades, the emergence of various modern fluorescence probe materials has promoted the rapid development of the fluorometries, typically including quantum dots [10], metal clusters [11], silicon or carbon dots [12,13], and fluorescent organic nanoparticles [14]. For example, Li et al. [15] prepared ultra-small fluorescent silver nanoclusters for probing Cu^{2+} ions based on the Cu^{2+}-induced quenching of fluorescence. A challenge regarding the environmental toxicity or non-degradable potential could, however, be commonly encountered for the current fluorescent materials like quantum dots. Therefore, developing new fluorescent probes with low toxicity and biodegradable property is of great interest for the fluorometric applications on a large scale. Dopamine (DA) as a composition of adhesive mussel foot proteins can present some unique physicochemical properties and excellent biocompatibility [16–22]. It can be polymerized to form the polymerized dopamine (PDA) to be applied in energy, environmental, and biomedical fields [16,18,19]. For example, PDA was coated onto magnetic particles to anchor phosphorylation-sensitive tyrosine probe for the electrochemical detection of organophosphates in blood [19]. The PDA nanoparticles were also employed as the green organic fluorescent probes for cell imaging [21] and the detection of metal ions like Fe^{3+} ions [22].

Moreover, graphene as a kind of hot nanomaterial has attracted the widespread interests due to it can possess many unique

* Corresponding author at: Shandong Province Key Laboratory of Life-Organic Analysis, College of Chemistry and Chemical Engineering, Qufu Normal University, Qufu, Shandong 273165, PR China.
E-mail addresses: huawang.qfnu@126.com, huawangqfnu@126.com (H. Wang).
[1] Web: http://wang.qfnu.edu.cn.

http://dx.doi.org/10.1016/j.snb.2016.03.142
0925-4005/

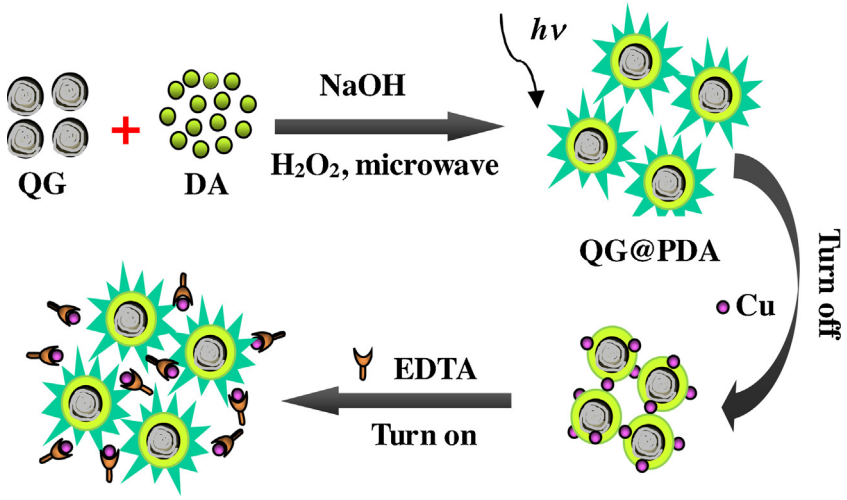

Scheme 1. Schematic illustration of the fabrication procedure of fluorescent QG@PDA nanocomposites by polymerizing DA onto the QG scaffolds under the microwave radiations, and the detection protocol for Cu^{2+} ions that could specifically "turn off" the fluorescence of QG@PDA nanocomposites, which could be further "turned on" by using the Cu^{2+} ligand of EDTA.

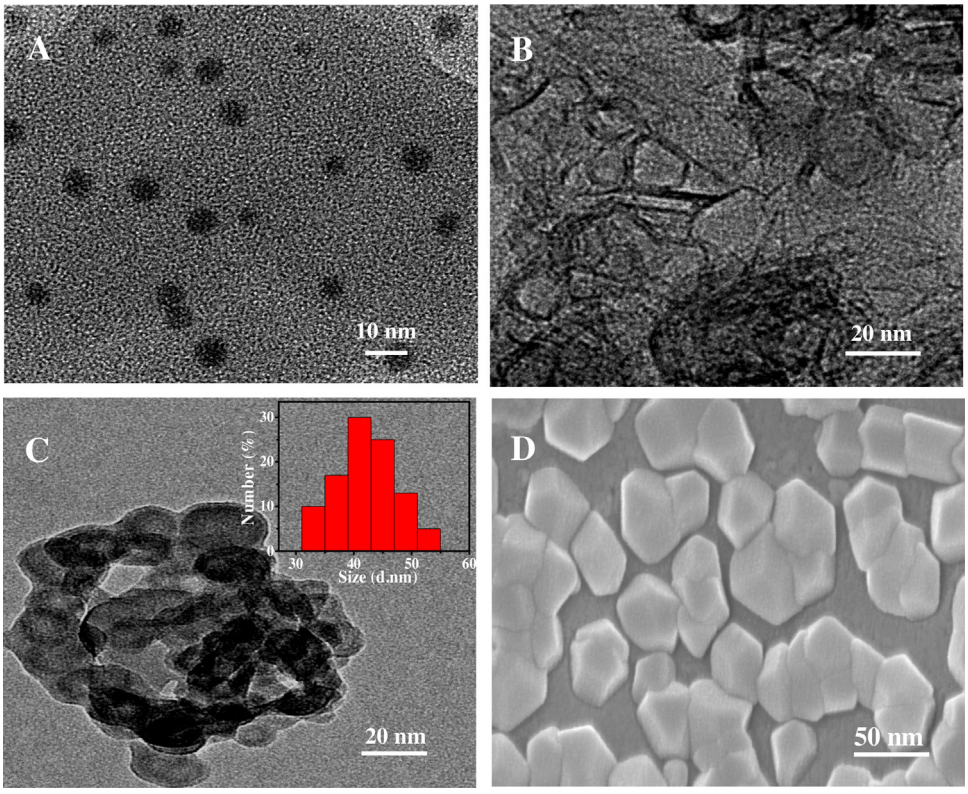

Fig. 1. TEM images of (A) PDA nanoparticles, (B) QG nanomaterials, (C) QG@PDA nanocomposites (Insert: the hydrodynamic diameters), and (D) SEM image of QG@PDA nanocomposites.

properties such as high electrical conductivity, thermal conductance, mechanical strength, and chemical stability [23]. In recent years, graphene or graphene oxide has been widely applied for electronics, environment, energy storage, and electrochemical sensors [24–27]. For example, Lin's group reported the application of N-doped graphene to achieve direct electron transfer kinetics for glucose oxidase [27]. They were also applied in the fluorescence sensors to serve as the quenchers of fluorescent probes [24,25,28]. For example, a fluorimetric analysis method was developed for probing Pb^{2+} ions by using graphene oxides to quench the fluorescence of functionalized CdSe/ZnS quantum dots [25]. To the best of our knowledge, however, graphene or its oxide has hardly been reported to act as the fluorescence booster so far. Recent years has witnessed the emergence of a new member of graphene family of Q-graphene (QG), known also as carbon quantum dot or nano-onion, which is hollow carbon nanomaterial consisting of multi-layer graphene and different types of carbon allotropes [29]. Up to date, nevertheless, QG nanomaterials with high proportion of folded edges and surface defects have been limited only for the elec-

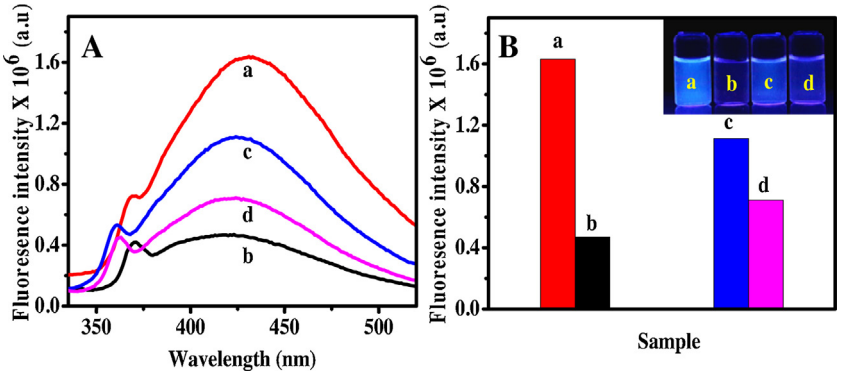

Fig. 2. Comparison of (A) the fluorescence spectra (λ_{ex} = 324 nm) and (B) the histograms of fluorescence intensities among (a) QG@PDA nanocomposites, (b) QG@PDA nanocomposites with Cu^{2+} ions, (c) PDA nanoparticles, and (d) PDA nanoparticles with Cu^{2+} ions (Insert: the corresponding photographs under UV light) by using QG@PDA nanocomposites or PDA nanoparticles (0.13 mM DA) and Cu^{2+} ions (50 μM).

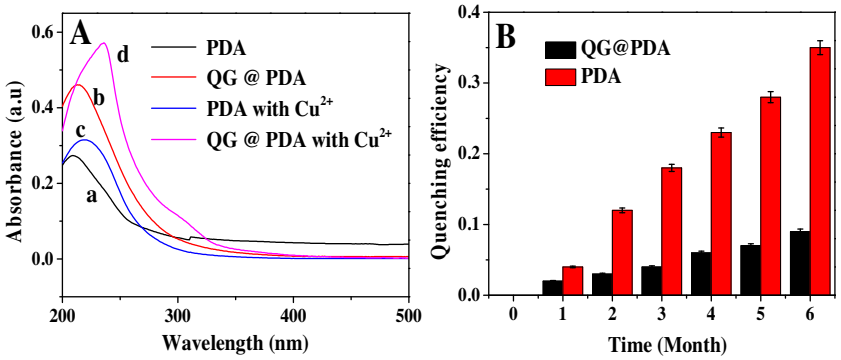

Fig. 3. (A) Comparison of UV–vis spectra between QG@PDA nanocomposites and PDA nanoparticles in the presence and absence of Cu^{2+} ions. (B) The changes of quenching efficiencies of QG@PDA nanocomposites and PDA nanoparticles stored at room temperature over different time intervals.

trochemical applications to facilitate the fast electron-transferring kinetics.

In the present work, nanospheric QG nanomaterials were employed for the first time as the new scaffolds for polymerizing PDA by the one-pot H_2O_2 oxidation under the microwave radiations, resulting in the fluorescent QG@PDA nanocomposites. Herein, the strong π-π stacking interactions between the benzene rings-containing PDA and hexatomic rings-containing QG scaffolds could endow the conjugated nanocomposites the high aqueous stability and photostability. More importantly, the greatly enhanced fluorescence of QG@PDA nanocomposites was unexpectedly observed, comparing to PDA nanoparticles alone. Moreover, the fluorescence of the resulting QG@PDA could be specifically quenched by Cu^{2+} ions. A rapid, selective, and ultrasensitive fluorimetric analysis method has thereby been developed for probing Cu^{2+} ions in wastewater. Systematic studies were conducted for the QG@PDA nanocomposites by using transmissions electron microscopy (TEM), scanning electronic microscopy (SEM), fluorescence spectrophotometer, UV–vis spectrophotometer, and fluorescence microscopy. The results indicate that the QG@PDA-based fluorimetric strategy can allow for the selective detections of Cu^{2+} ions in wastewater with high sensitivity and selectivity. Additionally, the quantitative observation for Cu^{2+} ions in samples was demonstrated by the fluorescence imaging.

2. Experimental section

2.1. Reagents and apparatus

Dopamine (DA) was obtained from Sangon Biotech Co., Ltd. (Shanghai, China). Q-Graphene (QG) nanomaterials were purchased from Graphene Supermarket (Calverton, United States). Hydrogen peroxide, ethylenediaminetetraacetate (EDTA), copper and other metal salts were purchased from Beijing Chemical Reagent Co. (Beijing, China). The wastewater samples from the local factory co-existing some other metal ions (i.e., Cr^{3+}, Fe^{3+}, Hg^{2+}, and Pb^{2+}) were spiked with Cu^{2+} ions of different concentrations. All chemicals used were of analytical grade and used directly without further purifications, and all glass containers were cleaned by aqua regia and water before usage.

The synthesis of QG@PDA fluorescent nanocomposites and PDA nanoparticles were performed using the microwave reactor

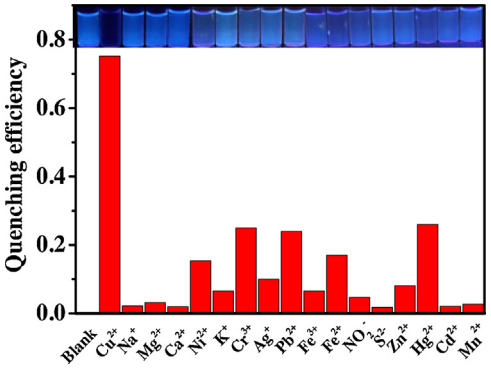

Fig. 4. Quenching efficiencies of QG@PDA nanocomposites (0.13 mM DA) in the presence of some co-existing ions indicated (50 μM) (Inset: the corresponding photographs under UV light), where F_0 and F correspond to the fluorescence intensities of QG@PDA nanocomposites in the absence and in the presence of possibly co-existing ions, respectively. The error bars represent the standard deviations of three replicated measurements.

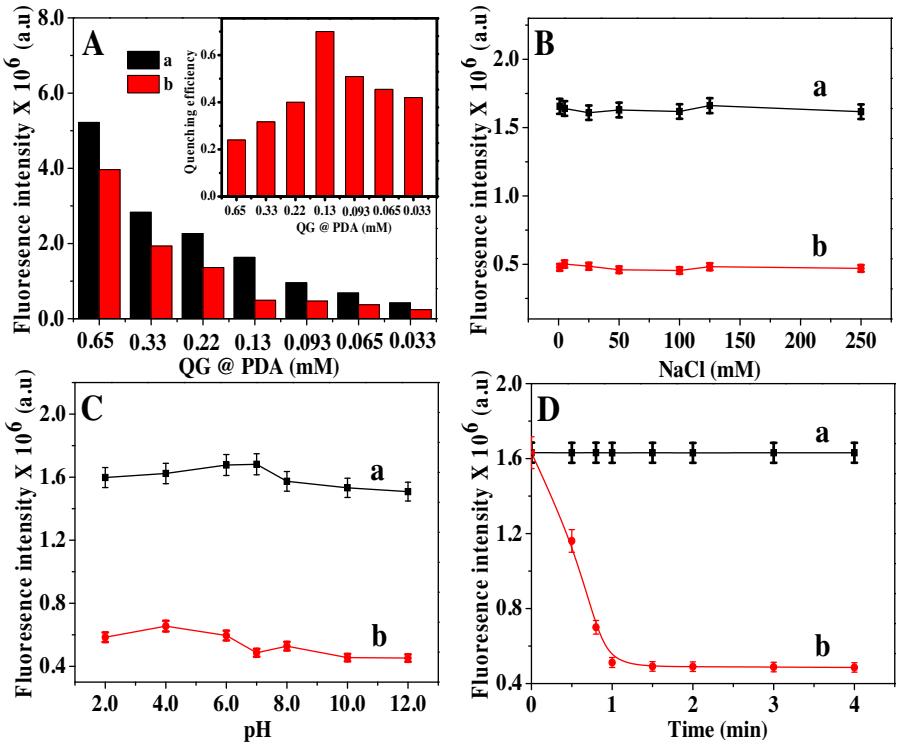

Fig. 5. Optimization of fluorometric detection conditions using QG@PDA nanocomposites of (A) the QG@PDA dosage-dependent fluorescence intensities (Inset: the quenching efficiencies), (B) the ion strength-dependent fluorescence intensities using different NaCl concentrations; (C) the pH-dependent fluorescence intensities, and (D) the reaction time-dependent change of fluorescence intensities of QG@PDA nanocomposites (0.13 mM of DA) in (a) absence and (b) presence of Cu^{2+} ions (50 μM).

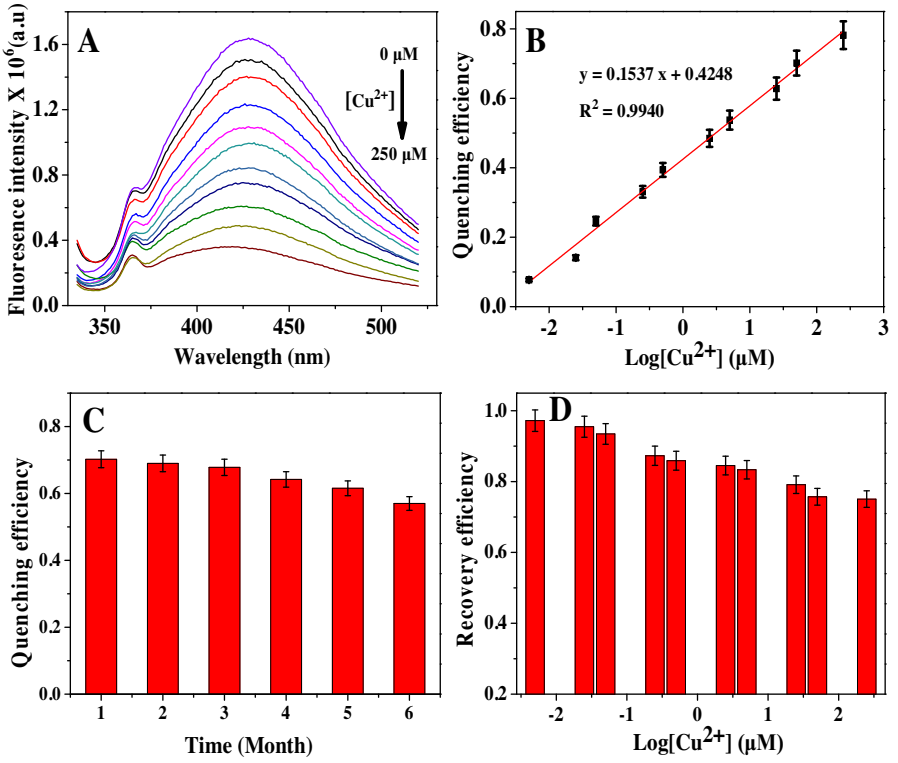

Fig. 6. (A) Fluorescence spectra of the QG@PDA nanocomposites in the presence of different concentrations of Cu^{2+} ions in water (0, 0.0050, 0.025, 0.050, 0.25, 0.50, 2.5, 5.0, 25, 50, 250 μM) (λ_{ex} = 324 nm); (B) the quenching efficiencies of QG@PDA nanocomposites versus the logarithmic concentrations of Cu^{2+} ions; (C) the fluorometric reproducibility for Cu^{2+} ions (50 μM) by using QG@PDA nanocomposites (0.13 mM of DA) that were stored over different time intervals; and (D) the recovery efficiencies of QG@PDA nanocomposites with Cu^{2+} ions of different concentrations by using EDTA (250 μM).

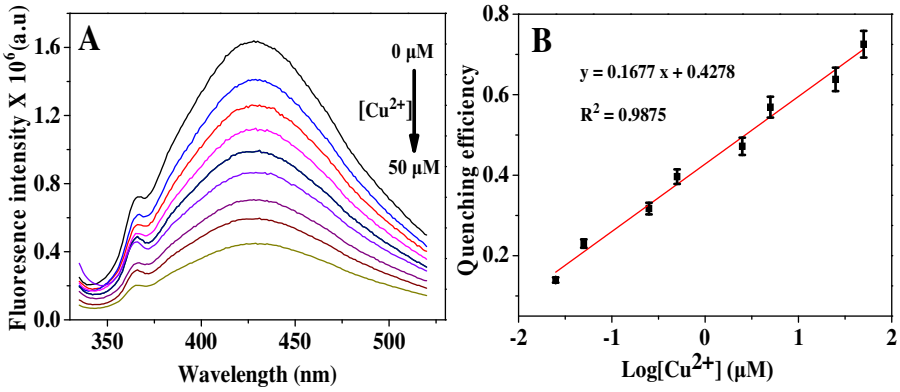

Fig. 7. (A) Fluorescence spectra (λ_{ex} = 324 nm) of QG@PDA nanocomposites (0.13 mM DA) in the presence of different concentrations of Cu^{2+} ions spiked in wastewater samples (0, 0.025, 0.050, 0.25, 0.50, 2.5, 5.0, 25, 50 μM); and (B) the relationship between the fluorescence quenching efficiencies versus the logarithmic concentrations of Cu^{2+} ions in wastewater samples.

(WBFY-205, China). The fluorescence measurements were conducted using fluorescence spectrophotometer (F-7000, Hitachi, Japan) operated at an excitation wavelength at 324 nm, with both excitations and emissions slit widths of 5.0 nm. The signals of fluorescence intensities were collected at 431 nm. UV–vis absorbance spectra were taken out using a UV–vis spectrophotometer (Shimadzu, UV-3600, Japan). The photographs of corresponding reactions products were recorded under UV light at 365 nm. Transmissions electron microscopy (TEM, Tecnai G20, FEI, USA), scanning electronic microscopy (SEM, Hitachi E-1010, Japan), and inverted fluorescence microscope (Olympus, IX73-DP80, Japan) were applied for the characterizations of different products.

2.2. Synthesis of fluorescent QG@PDA nanocomposites

The QG powder was dispersed in alcohol to be screened by centrifuging and then dried. An aliquot of QG nanomaterials (10 mg) was dissolved in 40 mL water, and then ultrasonically dispersed at room temperature for 30 min. Then, DA (100 mg) was introduced into the suspension to be further stirred for 30 min, followed by the addition of 3.3 mL NaOH (1.0 M). Furthermore, 6.7 mL H_2O_2 was dropped to react at 60 °C for 8 h under microwave radiations with the initial powers of 100 V. Subsequently, the products were centrifuged to remove any excessive unreacted QG nanomaterials including undesired PDA nanoparticles, yielding the fluorescent QG@PDA nanocomposites. Accordingly, the fluorescent PDA nanoparticles were synthesized except for the addition of QG nanomaterials.

2.3. The QG@PDA-based fluorimetry for Cu^{2+} ions

The fluorometric detections for Cu^{2+} ions were conducted simply by following the procedure. First, an aliquot (1.0 mL) of fluorescent QG@PDA nanocomposites (0.13 mM of DA) was mixed with 1.0 mL Cu^{2+} ions with different final concentrations (0, 0.0050, 0.025, 0.05, 0.25, 0.50, 2.5, 5.0, 25, 50, 250 μM). After being incubated at room temperature for 3 min, the fluorescence measurement was performed. The control tests for the common ions of Na^+, Mg^{2+}, Ca^{2+}, Ni^{2+}, K^+, Cr^{3+}, Ag^+, Pb^{2+}, Fe^{3+}, Fe^{2+}, NO_2^-, S^{2-}, Zn^{2+}, Hg^{2+}, Cd^{2+}, and Mn^{2+} ions (50 μM) were conducted accordingly. Moreover, an aliquot of EDTA (250 μM) was added to the reaction systems containing the QG@PDA nanocomposites and Cu^{2+} ions to examine the recovery of their fluorescence intensities. Subsequently, the developed fluorimetric assay was applied to detect the different concentrations of Cu^{2+} samples spiked in wastewater. The quenching efficiencies of QG@PDA nanocomposites by Cu^{2+} ions were calculated according to the equations: Quenching efficiencies = $(F_0-F)/F_0$, where F_0 and F refer to the fluorescence intensities of QG@PDA nanocomposites (λ_{ex} = 324 nm, λ_{em} = 431 nm) in the absence and presence of Cu^{2+} ions, respectively.

2.4. Fluorescence imaging for Cu^{2+} ions using QG@PDA nanocomposites

Optical fluorescent microscopy was employed to characterize the feasibility of fluorescence imaging of the QG@PDA nanocomposites. An aliquot of 5.0 μL QG@PDA suspensions (0.13 mM of DA) in the presence and absence of Cu^{2+} ions (50 μM) was dropped on a glass slide, with the PDA suspensions as the controls. After being dried in the room temperature, the fluorescent images were taken separately by using different optical filters of UV light (λ = 340–380 nm) and blue light (λ = 450–490 nm) for the excitation of photoluminescence.

3. Result and discussion

3.1. Synthesis and characterizations of QG@PDA nanocomposites

QG is a new hollow carbon nanosphere of multi-layer graphene with high proportion of folded edges and surface defects, which has been demonstrated to enable the fast electron transfer kinetics [29]. Here, the QG nanomaterials were alternatively employed as the scaffolds for loading PDA to form the fluorescent QG@PDA nanocomposites. The typical fabrication procedure is schematically illustrated in Scheme 1. Under the alkaline and microwave-radiation conditions, DA was one-pot polymerized onto the QG scaffold by the H_2O_2 oxidation. The morphological structure of the resulting QG@PDA nanocomposites was characterized by TEM imaging (Fig. 1). It was observed that PDA nanoparticles alone could be formed uniformly with the average particle size of about 8.0 nm in diameter (Fig. 1A), in contrast to the ones reported elsewhere [21]. The QG nanomaterials could display varying sizes of about 20–30 nm (Fig. 1B). The QG@PDA nanocomposites could be yielded with the clear core-shell structure (Fig. 1C), showing the average of hydrodynamic diameters of about 44 nm, as determined by the dynamic light scattering (Fig. 1C, Insert). Moreover, as can be seen from the SEM image in Fig. 1D, a very smooth surface morphology was observed for QG@PDA nanocomposites, demonstrating that PDA might be coated on the QG scaffolds with a dense and stable configuration. More importantly, the as-prepared QG@PDA nanocomposites could thereby achieve the high aqueous stability, photostability, and enhanced fluorescence, as demonstrated afterwards.

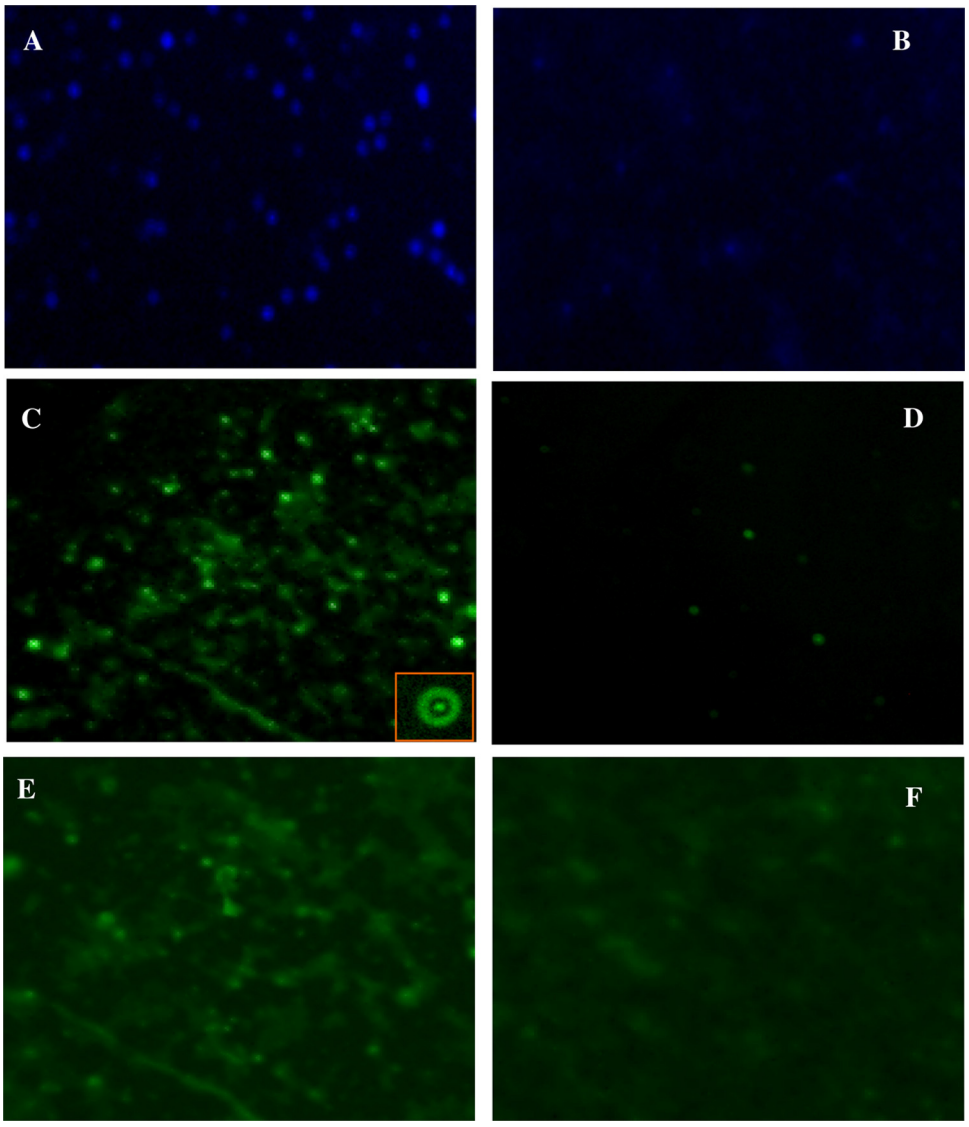

Fig. 8. Fluorescence microscopy images of the QG@PDA nanocomposites in the (A and C) absence and (B and D) presence of Cu^{2+} ions, in comparison to PDA nanoparticles (E) without and (F) with Cu^{2+} ions. The fluorescence images were taken separately by using two optical filters of UV light (A and B) and blue light (C, D, E, and F) for the photoluminescence excitation, where the samples were dropped on the glass slides and further dried at the room temperature. The amplified image of QG@PDA nanocomposite was shown (C**,** Insert). (For interpretation of the references to colour in this figure legend, the reader is referred to the web version of this article.).

3.2. Studies on the interactions between QG@PDA nanocoposites and Cu^{2+} ions

The interactions between the fluorescent QG@PDA nanocomposites and Cu^{2+} ions were examined, with the testing procedure schematically illustrated in Scheme 1. Here, the fluorescence of QG@PDA nanocomposites could be rationally "turned off" by Cu^{2+} ions, which would be further "turned on" if the strong Cu^{2+}-chelating ligand of EDTA was introduced. Fig. 2 shows the comparison of the Cu^{2+} quenching efficiencies between the QG@PDA nanocomposites and PDA nanoparticles. As can be seen from Fig. 2A, the emission spectra of QG@PDA nanocomposites and PDA nanoparticles could peak at 424 nm and 431 nm, respectively, showing a little shift in the fluorescence emissions. Remarkably, the fluorescence intensity of QG@PDA nanocomposites (curve a) was about 1.5-time higher than that of PDA nanoparticles (curve c), as visually observed from their photographs (Fig. 2B). Also, larger Cu^{2+}-induced quenching of fluorescence intensities could be obtained for the QG@PDA nanocomposites. In addition, both of QG@PDA nanocomposites or PDA nanoparticles could display the tunable photoluminescence (data not shown), presumably due to the relatively wide size distribution of PDA resulting from the uncontrollable polymerization of DA and oxidation of PDA [21]. Therefore, the introduction of QG scaffolds could dramatically enhance the fluorescence of PDA by forming QG@PDA nanocomposites, which is in contrast to the common graphene materials that generally serve as the fluorescence quenchers [24,25,28]. Although the detailed reasons remain unknown at present, the high proportion of folded edges and surface defects of QG scaffolds, which would conduct the strong π-π stacking interactions with the PDA coatings, is speculated to play a vital role in the QG-triggered enhancement of the fluorescence of QG@PDA nanocomposites. Importantly, under the harsh fabrication conditions of the microwave-aided H_2O_2 oxidization, the internal configuration and the exterior compositions including the surface defects of QG might be changed. Particularly, more —OH groups of electronic donors could be thus produced on the QG surface to facilitate the enhanced fluorescence of the coated PDA through the "electron-donor effect" [30]. In addition, semiconductive QD might conduct the enhancement of an evanescence wave and the

wave-guiding nature for the fluorescent coatings, as reported elsewhere for some metal oxides (i.e., ZnO) [31–35]. Accordingly, QG with the spherical hollow structure can present some special properties different from the common graphene with the planar structure, of which the QG-enabled enhancement of PDA fluorescence here might serve as an example. Nevertheless, the detailed mechanism remains unclear at present, on which a further investigation is undergoing in our group.

Furthermore, a comparison of UV–vis spectra between the QG@PDA nanocomposities and PDA nanoparticles was performed in the presence and absence of Cu^{2+} ions (Fig. 3A). It was found that the QG@PDA nanocomposites could show the absorbance peak at 220 nm (curve b), which would shift to 235 nm after the addition of Cu^{2+} ions (curve d). Meanwhile, PDA nanoparticles could present the absorbance peak at 210 nm (curve a), which would shift to 216 nm after introducing Cu^{2+} ions (curve c). Of note, the UV–vis absorbances could increase for both of the PDA and QG@PDA fluorescent materials after the addition of Cu^{2+} ions, implying that they might presumably agglomerate upon binding with Cu^{2+} ions. Importantly, the QG@PDA nanocomposites could again present the relatively bigger difference of UV–vis absorbance between the presence and absence of Cu^{2+} ions, in consistence with those in the Cu^{2+}-quenching fluorescence intensities aforementioned. Moreover, Fig. 3B manifests the comparison of storage stability between the fluorescent QG@PDA nanocomposites and PDA nanoparticles, where the quenching efficiencies were calculated. Obviously, the fluorescence of QG@PDA nanocomposites could survive in water over six months with no significant change of fluorescence intensities. In contrast, the fluorescence of PDA nanoparticles might fade away during the testing time. Also, no significant photobleaching was observed during the continuous excitation at 365 nm for 1 h (data not shown), showing the potential of imaging applications. Therefore, the QG scaffolds might endow the coated PDA fluorogens with the considerably high aqueous stability and photostability, which was thought to result from the strong π-π stacking interactions between the benzene rings-containing PDA and hexatomic rings-containing QG scaffolds. Additionally, QG, as a new kind of graphene material with the hollow structure and high surface-to-volume ratio, could possess so strong adsorption for PDA that PDA could be coated onto them with highly dense and stable configuration, as clearly manifested in the SEM image in Fig. 1D.

The fluorescent responses of QG@PDA nanocomposites to other kinds of co-existing ions were investigated, mainly including Na^{+}, Mg^{2+}, Ca^{2+}, Ni^{2+}, K^{+}, Cr^{3+}, Ag^{+}, Pb^{2+}, Fe^{3+}, Fe^{2+}, NO^{2-}, S^{2-}, Zn^{2+}, Hg^{2+}, Cd^{2+}, and Mn^{2+} ions (Fig. 4). As expected, only Cu^{2+} ions could immediately trigger the quenching of the fluorescence emissions of QG@PDA nanocomposites, as apparently shown in the corresponding photographs (Fig. 4, Insert). Accordingly, the QG@PDA nanocomposites could serve as the robust fluorescent probes for the selective Cu^{2+} detections. Herein, the phenomenon of the selective fluorescence quenching of QG@PDA nanocomposites caused by Cu^{2+} ions was thought to result from the specific chelating between Cu^{2+} ions and the $-NH_2$ and —OH groups of PDA shells of QG@PDA nanocomposites, as also disclosed for other kinds of fluorescent materials [9,11]. More importantly, the Cu^{2+}-induced fluorescence quenching could be restored by introducing an adequate amount of stronger Cu^{2+}-chelating ligands like EDTA to allow for the evaluation of reversible fluorescence as demonstrated afterwards. It is worthy to point out that most of common metal ions (i.e., Na^{+}, Mg^{2+}, Ca^{2+}, and K^{+} ions) might display negligible interference for the detection of Cu^{2+} ions even at the concentrations 100 fold higher than that of Cu^{2+} ions (data not shown). However, some heavy metal ions like Ni^{2+}, Cr^{3+}, Pb^{2+}, Fe^{2+}, and Hg^{2+} ions could to some degree cause the fluorescence quenching of QG@PDA nanocomposites at over 10 fold higher concentrations, of which the quenched fluorescence could not be restored by EDTA. Accordingly, with respect to the samples co-existing other heavy metal ions with too high concentrations, the selective detection of Cu^{2+} ions should be realized by measuring the EDTA-enabled restoration efficiencies of quenched fluorescence.

3.3. Optimization of main sensing conditions of QG@PDA-based fluorimetry for Cu^{2+} ions

The QG@PDA-based fluorimetry for Cu^{2+} ions was investigated depending on the QG@PDA dosages that were calculated from different DA concentrations (Fig. 5A). It is found that the decreasing QG@PDA dosages could result in the decrease in the change of fluorescence intensities quenched by Cu^{2+} ions. However, their quenching efficiencies of fluorescence could vary for the different QG@PDA dosages so as to reach the maximum at QG@PDA nanocomposites of 0.13 mM in DA (Fig. 5A, Insert), which would be selected as the optimal one thereafter. Moreover, Fig. 5B shows the effects of ionic strengths on the QG@PDA-based fluorometric analysis of Cu^{2+} ions using different NaCl concentrations. Accordingly, no significant influence of ionic strengths (up to 250 mM NaCl) was observed on the fluorescence intensities of QG@PDA nanocomposites in the presence and absence of Cu^{2+} ions, indicating that the electrostatic interaction might present little influence. Furthermore, the pH-dependent fluorimetric responses of QG@PDA nanocomposites to Cu^{2+} ions were explored, with the results shown in Fig. 5C. Obviously, the optimal pH value for the Cu^{2+} sensing should be at pH 7.0. In addition, the fluorimetric response time of QG@PDA nanocomposites to Cu^{2+} ions was evaluated (Fig. 5D). Accordingly, the fluorescence intensities of QG@PDA nanocomposites decreased drastically upon the addition of Cu^{2+} ions and tended to be stable after 2 min (curve b), indicating that a fast fluorescence response to Cu^{2+} ions could be expected.

3.4. Sensing performances of the QG@PDA-based fluorimetry for Cu^{2+} ions

Under the optimal conditions, the developed QG@PDA-based fluorimetry was applied for the detection of Cu^{2+} ions in water (Fig. 6). The fluorescent spectras of QG@PDA nanocomposites with Cu^{2+} ions of different concentrations were manifested in Fig. 6A. One can observe that the fluorescence intensities could rationally decrease as Cu^{2+} concentrations increased. Fig. 6B describes the relationship between the fluorescence quenching efficiencies and the logarithms of Cu^{2+}concentrations. Accordingly, Cu^{2+} ions could be detected over the linear concentrations ranging from 5.0 nM to 250 μM ($R^2 = 0.9940$), with the limit of detection (LOD) of 1.25 nM, estimated by the 3σ rule. Moreover, the continuous fluorimetric detections for Cu^{2+} ions were conducted by using QG@PDA nanocomposites that were stored over different time intervals of six months (Fig. 6C). The results indicate that the Cu^{2+}-induced quenching efficiencies might show not significant change over time. Therefore, the developed fluorometry for Cu^{2+} ions could exhibit the high analysis reproducibility, presumably resulting from the pretty high aqueous stability of QG@PDA nanocomposites aforementioned. Furthermore, the recoveries of the Cu^{2+}-quenched fluorescence of QG@PDA nanocomposites were explored by using the Cu^{2+} chelating ligand of EDTA (Fig. 6D). Compared to the corresponding fluorescence intensities in Fig. 6A, the EDTA-restored percents of the fluorescence intensities were found to be 75%–98%, depending on the amounts of Cu^{2+} ions used in the reactions. Accordingly, it is inferred that the Cu^{2+}-induced fluorescence quenching of the QG@PDA nanocomposites might occur by the common energy transfer, which might not damage the PDA shells of QG@PDA nanocomposites. Importantly, the reversible fluorescence quenched by Cu^{2+} ions could be expected to ensure the high selectivity of the QG@PDA-based fluorimetry for Cu^{2+} ions

especially in the wastewater samples co-existing other metal ions (i.e., Hg^{2+} and Pb^{2+} ions) with too high levels.

3.5. The QG@PDA-based fluorimetric analysis and fluorescence imaging for Cu^{2+} samples

The application feasibility of the QG@PDA-based fluorimetry was investigated for probing Cu^{2+} ions spiked in the wastewater samples (Fig. 7). As shown in Fig. 7A, the additions of Cu^{2+} ions could lead to the rationally decrease in the fluorescence intensities of QG@PDA nanocomposites. A relationship between the quenching efficiencies and the logarithms of the concentrations of Cu^{2+} ions was obtained in the linear ranges from 25 nM to 50 μM (R^2 = 0.9875), with the LOD of about 10 nM (Fig. 7B). Of note, this LOD is different from the one for Cu^{2+} ions in water because of the different sample backgrounds of co-existing metal ions. In view of the practical applications, it should be considered as the one for the proposed method. Moreover, the LOD of the QG@PDA-based fluorimetry is lower than those of some other fluorimetric (about 160 nM) and colorimetric (about 50 μM) analysis methods reported elsewhere [35,36]. Also, the detection range of the developed fluorimetry is much wider than those of the previous fluorimetric (0.20–8.0 μM) and colorimetric (50–500 μM) ones mentioned.

Moreover, the quantitative observation by the QG@PDA-based fluorescence imaging for Cu^{2+} ions was investigated using the fluorescent microscopy, taking PDA nanoparticles for comparison (Fig. 8). Two types of blue and green photoluminescences were observed for QG@PDA nanocomposites with the core-shell structure (Fig. 8C, Insert), which were excited separately by the optical filters of UV light (Fig. 8A) and blue light (Fig. 8C), showing the excitation-dependent tunable photoluminescence. Moreover, both of the blue and green photoluminescences could be efficiently quenched by Cu^{2+} ions as shown in Fig. 8B and D, respectively. More importantly, under the blue-light excitation, the green photoluminescence of QG@PDA nanocomposites (Fig. 8C) is much brighter than that of PDA nanoparticles (Fig. 8E). Also, the Cu^{2+}-induced photoluminescence quenching of QG@PDA nanocomposites (Fig. 8D) could be more efficient than that of PDA nanoparticles (Fig. 8F). These results above indicate that the QG@PDA nanocomposites could be applied for the visual quantification by fluorescence imaging for Cu^{2+} ions in water samples as well as other kind of samples like plants and aquatic products.

4. Conclusion

In summary, nanospheric QG nanomaterials were successfully applied as the scaffolds for polymerizing PDA under the microwave radiations. The resulting fluorescent QG@PDA nanocomposites could present considerably high aqueous stability and photostability, which was thought to result from the strong π-π stacking interactions between the benzene rings-containing PDA and hexatomic rings-containing QG scaffolds. Unexpectedly, the QG scaffolds could act as the fluorescent promoter so as to endow the QG@PDA nanocomposites with enhanced fluorescence and photoluminescence, in contrast to the common graphene materials that were generally reported to serve as the fluorescence quenchers. Moreover, their fluorescence and photoluminescence could be specifically quenched by Cu^{2+} ions through the specific chelating interaction between Cu^{2+} ions and the $-NH_2$ and $-OH$ groups of PDA shells of QG@PDA nanocomposites, which might be restored by using the strong Cu^{2+}-chelating ligand of EDTA. The so developed QG@PDA-based fluorimetry could allow for the detection of Cu^{2+} ions in wastewater samples with high detection sensitivity and selectivity. The practical feasibility of the quantitative observation by the fluorescence imaging for Cu^{2+} ions in wastewater was also demonstrated. The fabricated fluorescent nanocomposites may find the extensive applications for the fluorimetric analysis of Cu^{2+} ions in wastewater, plants, and aquatic products.

Acknowledgements

This work is supported by the National Natural Science Foundations of China (No. 21375075 and 21302109), the “spark program” of the Ministry of Science and Technology (No. 2015GA105005), and the Taishan Scholar Foundation of Shandong Province, PR China.

References

[1] B. Sarkar, Treatment of Wilson and Menkes diseases, Chem. Rev. 99 (1999) 2535–2544.
[2] P. Dusek, P.M. Roos, T. Litwin, S.A. Schneider, T.P. Flaten, J. Aaseth, The neurotoxicity of iron, copper and manganese in Parkinson’s and Wilson’s diseases, J. Trace Elem. Med. Biol. 31 (2015) 193–203.
[3] K. Yin, B.W. Li, X.C. Wang, W.W. Zhang, L.X. Chen, Ultrasensitive colorimetric detection of Cu^{2+} ion based on catalytic oxidation of L-cysteine, Biosens. Bioelectron. 64 (2015) 81–87.
[4] Y.R. Ma, H.Y. Niu, Y.Q. Cai, Colorimetric detection of copper ions in tap water during the synthesis of silver/dopamine nanoparticles, Chem. Commun. 47 (2011) 12643–12645.
[5] T.S. Seeger, F.C. Rosa, C.A. Bizzi, V.L. Dressler, E.M. Flores, F.A. Duarte, Feasibility of dispersive liquid–liquid microextraction for extraction and preconcentration of Cu and Fe in red and white wine and determination by flame atomic absorption spectrometry, Spectrochim. Acta B 105 (2015) 136–140.
[6] S. Takano, M. Tanimizu, T. Hirata, Y. Sohrin, Determination of isotopic composition of dissolved copper in seawater by multi-collector inductively coupled plasma mass spectrometry after pre-concentration using an ethylenediaminetriacetic acid chelating resin, Anal. Chim. Acta 784 (2013) 33–41.
[7] M. Liu, Y.H. Feng, C.H. Zhang, G.F. Wang, B. Fang, Electrochemical determination of copper (ii) using co-poly (cupferron and β-naphthol)/gold nanoparticles modified glassy carbon electrodes, Anal. Methods 3 (2011) 1595–1600.
[8] J.B. Wang, Q.S. Zong, A new turn-on fluorescent probe for the detection of copper ion in neat aqueous solution, Sens. Actuators B Chem. 216 (2015) 572–577.
[9] N. Zhang, Y.M. Si, Z.Z. Sun, L.J. Chen, R. Li, Y.C. Qiao, H. Wang, Rapid, selective, and ultrasensitive fluorimetric analysis of mercury and copper levels in blood using bimetallic gold–silver nanoclusters with silver effect-enhanced red fluorescence, Anal. Chem. 86 (2014) 11714–11721.
[10] F.X. Wang, Z.Y. Gu, W. Lei, W.J. Wang, X.F. Xia, Q.L. Hao, Graphene quantum dots as a fluorescent sensing platform for highly efficient detection of copper(II) ions, Sens. Actuators B Chem. 190 (2014) 516–522.
[11] J. Liu, X.L. Ren, X.W. Meng, Z. Fang, F.Q. Tang, Sensitive and selective detection of Hg^{2+} and Cu^{2+} ions by fluorescent Ag nanoclusters synthesized via a hydrothermal method, Nanoscale 5 (2013) 10022–10028.
[12] J.H. Warner, A. Hoshino, K. Yamamoto, R. Tilley, Water-soluble photoluminescent silicon quantum dots, Angew. Chem. Int. Ed. 117 (2005) 4626–4630.
[13] Y.P. Sun, B. Zhou, Y. Lin, W. Wang, K.S. Fernando, P. Pathak, M.J. Meziani, B.A. Harruff, X. Wang, H.F. Wang, Quantum-sized carbon dots for bright and colorful photoluminescence, J. Am. Chem. Soc. 128 (2006) 7756–7757.
[14] J.A. Cotruvo Jr., A.T. Aron, K.M. Ramos Torres, C.J. Chang, Synthetic fluorescent probes for studying copper in biological systems, Chem. Soc. Rev. 44 (2015) 4400–4414.
[15] S.L. Li, W.P. Cao, A. Kumar, S.B. Jin, Y.Y. Zhao, C.Q. Zhang, G.Z. Zou, P.C. Wang, F. Li, X.J. Liang, Highly sensitive simultaneous detection of mercury and copper ions by ultrasmall fluorescent DNA–Ag nanoclusters, New J. Chem. 38 (2014) 1546–1550.
[16] Y.R. Ma, X.L. Zhang, T. Zeng, D. Cao, Z. Zhou, W.H. Li, H.Y. Niu, Y.Q. Cai, Polydopamine-coated magnetic nanoparticles for enrichment and direct detection of small molecule pollutants coupled with MALDI-TOF-MS, ACS Appl. Mater. Interfaces 5 (2013) 1024–1030.
[17] G. Yeroslavsky, M. Richman, L. Dawidowicz, S. Rahimipour, Sonochemically produced polydopamine nanocapsules with selective antimicrobial activity, Chem. Commun. 49 (2013) 5721–5723.
[18] K.J. Jeong, L.Q. Wang, C.F. Stefanescu, M.W. Lawlor, J. Polat, C.H. Dohlman, R.S. Langer, D.S. Kohane, Polydopamine coatings enhance biointegration of a model polymeric implant, Soft Matter 7 (2011) 8305–8312.
[19] Y.M. Si, N. Zhang, Z.Z. Sun, S. Li, L.Y. Zhao, R. Li, H. Wang, A phosphorylation-sensitive tyrosine-tailored magnetic particle for electrochemically probing free organophosphates in blood, Analyst 139 (2014) 5466–5471.

[20] Y.L. Liu, K.L. Ai, L.H. Lu, Polydopamine and its derivative materials: synthesis and promising applications in energy, environmental, and biomedical fields, Chem. Rev. 114 (2014) 5057–5115.
[21] X.Y. Zhang, S.Q. Wang, L.X. Xu, L. Feng, Y. Ji, L. Tao, S.X. Li, Y. Wei, Biocompatible polydopamine fluorescent organic nanoparticles: facile preparation and cell imaging, Nanoscale 4 (2012) 5581–5584.
[22] J.H. Lin, C.J. Yu, Y.C. Yang, W.L. Tseng, Formation of fluorescent polydopamine dots from hydroxyl radical-induced degradation of polydopamine nanoparticles, Phys. Chem. Chem. Phys. 17 (2015) 15124–15130.
[23] Q. Tang, Z. Zhou, Z.F. Chen, Graphene-related nanomaterials: tuning properties by functionalization, Nanoscale 5 (2013) 4541–4583.
[24] F. Perreault, A.F. De Faria, M. Elimelech, Environmental applications of graphene-based nanomaterials, Chem. Soc. Rev. 44 (2015) 5861–5896.
[25] M. Li, X.J. Zhou, S.W. Guo, N.Q. Wu, Detection of lead (II) with a turn-on fluorescent biosensor based on energy transfer from CdSe/ZnS quantum dots to graphene oxide, Biosens. Bioelectron. 43 (2013) 69–74.
[26] Y. Wu, Z. Wen, H. Feng, J. Li, Sucrose-assisted loading of $LiFePO_4$ nanoparticles on graphene for high-performance lithium-ion battery cathodes, Chem. Eur. J. 19 (2013) 5631–5636.
[27] Y. Wang, Y. Shao, D.W. Matson, J. Li, Y. Lin, Nitrogen-doped graphene and its application in electrochemical biosensing, ACS Nano 4 (2010) 1790–1798.
[28] D.A. Brownson, D.K. Kampouris, C.E. Banks, Graphene electrochemistry: fundamental concepts through to prominent applications, Chem. Soc. Rev. 41 (2012) 6944–6976.
[29] E.P. Randviir, D.A. Brownson, M. Gómez Mingot, D.K. Kampouris, J. Iniesta, C.E. Banks, Electrochemistry of Q-graphene, Nanoscale 4 (2012) 6470–6480.
[30] S.Y. Li, Z.Z. Sun, R. Li, M.M. Dong, L.Y. Zhang, W. Qi, X.L. Zhang, H. Wang, ZnO nanocomposites modified by hydrophobic and hydrophilic silanes with dramatically enhanced tunable fluorescence and aqueous ultrastability toward biological imaging applications, Sci. Rep. 19 (2015) 169–171.
[31] S.Y. Li, M.M. Dong, R. Li, L.Y. Zhang, Y.C. Qiao, Y. Jiang, W. Qi, H. Wang, A fluorometric microarray with ZnO substrate enhanced fluorescence and suppressed coffee ring effects for fluorescence immunoassays, Nanoscale 7 (2015) 18453–18458.
[32] V. Adalsteinsson, O. Parajuli, S. Kepics, A. Gupta, W.B. Reeves, J. Hahm, Ultrasensitive detection of cytokines enabled by nanoscale ZnO arrays, Anal. Chem. 80 (2008) 6594–6601.
[33] M. Singh, S. Song, J. Hahm, Unique temporal and spatial biomolecular emission profile on individual zinc oxide nanorods, Nanoscale 6 (2014) 308–315.
[34] R. Kaiser, Y. Levy, N. Vansteenkiste, A. Aspect, W. Seifert, D. Leipold, J. Mlynek, Resonant enhancement of evanescent waves with a thin dielectric waveguide, Opt. Commun. 104 (1994) 234–240.
[35] P.S. Song, Y. Xiang, R.R. Wei, A.J. Tong, A fluorescent chemosensor for Cu^{2+} detection in solution based on aggregation-induced emission and its application in fabricating Cu^{2+} test papers, J. Lumin. 53 (2014) 215–220.
[36] Y. Zhou, S.X. Wang, K. Zhang, X.Y. Jiang, Copper (II) by azide-and alkyne-functionalized gold nanoparticles using click chemistry, Angew. Chem. 120 (2008) 7564–7566.

Biographies

Minmin Dong received her bachelor degree in Chemistry Application from the QuFu Normal University China, in 2013, and now is a postgraduate student in Analytical Chemistry at the same university. Her research interests include Biosensors and Medical Detectors R&D.

Chunli Liu received her bachelor degree in Chemical Engineering and Technology from the QuFu Normal University, China, in 2013, and now is a postgraduate student in Analytical Chemistry at the same university. Her research interests include Biosensors and Medical Detectors R&D.

Shuying Li received her bachelor degree in Chemical Engineering and Technology from the QuFu Normal University, China, in 2013, and now is a postgraduate student in Analytical Chemistry at the same university. Her research interests include Biosensors and Medical Detectors R&D.

Rui Li received her bachelor degree in Chemical Education from the QuFu Normal University, China, in 2013, and now is a postgraduate student in Analytical Chemistry at the same university. Her research interests include Biosensors and Medical Detectors R&D.

Yuchun Qiao received her bachelor degree in Chemical Engineering and Technology from the QuFu Normal University, China, in 2014, and now is a postgraduate student in Analytical Chemistry at the College of Chemistry and Chemical Engineering in the same university. His research interests mainly include Biosensors and Medical Detectors R&D.

Liyan Zhang received her bachelor degree in Chemistry Education from the QuFu Normal University in China, in 2014, and now is a postgraduate student in Analytical Chemistry at the same university. Her research interests include Biosensors and Medical Detectors R&D.

Wei Wei received his ph.D from Chengdu Institute of biology, Chinese Academy of Sciences, China, in 2012, and now is working at Qufu Normal University as an associate professor in Chemistry. His research interests mainly include Organic Chemistry

Wei Qi received her ph.D from Chinese Academy of Sciences, China, in 2009, and now is working at Qufu Normal University as an associate professor in Chemistry. Her research interests mainly include Colloid and Interface Chemistry.

Hua Wang received his ph.D from Hunan University, China, in 2004, and now is working at Qufu Normal University as a professor in Chemistry. His research interests mainly include Chemo/Biosensors, Advanced Functional Materials, and Organic Synthesis.